Hygrothermal Modeling of Green Roof Made with Substrate and Drainage Layers of Coarse Recycled Materials

Mostafa Kazemi, Luc Courard, Shady Attia
Department UEE, Faculty of Applied Sciences, Université de Liège, Liège, Belgium.

Abstract

The thermal performance of an extensive green roof can be influenced by the initial hygrothermal conditions of substrate and drainage layers. Moreover, coarse recycled materials can affect the thermal resistance of green roof layers, while there is a demand for optimizing their thickness. Therefore, the main objective of this study is to optimize the thickness of green roof layers, once coarse recycled materials were used for substrate and drainage layers: WUFI software has been used for such application, which was suitable for modeling the initial hygrothermal conditions (heat and moisture properties) of green roof layers. According to the results, R_c-value for the green roof without coarse recycled materials was found slightly higher than that of the specimen with coarse recycled materials (4.1%), indicating nearly the same thermal resistance of the former and the latter. The green roof model with 15-cm substrate and 6-cm drainage layer can be regarded as the best appropriate system concerning their better thermal resistance and lower weight.

Key Innovations

- Thermal resistance of green roof layers with coarse recycled materials was experimentally assessed concerning ISO 9869-1 (2014).
- Thermal performance of substrate and drainage layers was simulated by considering their initial hygrothermal conditions.
- Thickness of green roof layers was optimized.

Practical Implications

For green roof layers in wet condition, the simultaneous effect of heat and moisture properties of materials must be considered to validate the models reliably and assess the their thermal performance reliably.

Introduction

The energy consumption of houses and building sectors has raised some concerns, accounting for 40% of total primary energy demand in the European Union (Coma et al., 2014). Therefore, the reduction of energy demand in this area is a priority in the construction industry to enhance new structures' insulation dynamic. Some researchers have proposed the replacement of common flat roofs with green roofs to improve the performance and energy savings in the building sector (Coma et al., 2016). There are three major types of green roof: intensive, semi-intensive and extensive green roofs. Among different types of green roofs, the extensive green roof has shallow substrate layer and require less maintenance; so, it has been proposed to be used in the building sector (Kuppusamy Vijayaraghavan, 2016).

From the top to down, the extensive green roof layers include vegetation, growing medium (substrate), filter, and drainage and insulation layers (Tabares-Velasco et al., 2012). Researchers have proposed to use the polyethylene modular panel (egg-carton-shaped panel) as drainage layer of green roof (Chenani et al., 2015; Dvorak & Volder, 2013; Jim, 2014; Mickovski et al., 2013; Vesuviano & Stovin, 2013). However, this modular panel has been replaced with natural aggregates in some cases (Wanielista et al., 2008). In this regard, Wanielista and Hardin (Wanielista et al., 2008) performed a comparison between the use of polyethylene modular panel and natural gravel aggregate in the drainage layer. The results showed that the quality of water leaked from the natural gravel aggregate was nearly the same as that leaked from the polyethylene modular panel. Moreover, the evapotranspiration process in the green roof with the natural gravel aggregate as the drainage layer increased by increasing the atmospheric temperature.

Although the drainage layer with natural aggregates can be considered as a permeable layer, which is very important for the leakage of water from the green roof (Uhl & Schiedt, 2008; K. Vijayaraghavan et al., 2012), the overuse of natural aggregate in the construction sector has harmed the environment in recent decades (Vila et al., 2012). This issue can be somewhat solved by replacing natural aggregates with recycled materials in the green roofs. The green roofs' water retention capacity can be improved using recycled materials in the substrate and drainage layers. Besides, the high porosity of recycled materials can lead to accelerating the leakage of extra water from the green roof (Kazemi et al., 2020; Nematzadeh et al., 2020); in this regard, a study by Berndtsson et al. (2006) on the extensive green roofs showed that the crushed brick as a drainage layer slightly retained small particles, released from the soil, and somewhere prevented washing them away. Recently, the thermal performance of green roof with the drainage layer of perlite, expanded clay, and rubber crumbs was assessed by Cascone et al. (2018). According to these results, the diurnal temperature fluctuations of buildings with the green roof decreased compared to that with the traditional roof, owing to higher thermal inertia generated by the drainage layer and substrate. Another study by Coma et al. (2016) showed that, during the summer, the green roof with rubber crumbs provided more energy savings than volcanic gravel as a drainage layer in the green roof.

To simulate thermal and moisture distribution, the modeling tools have been widely used by researchers and a list of hygrothermal simulation software was provided by Delgado et al. (2012) to apply to building physics. Some hygrothermal simulation tools have met the criteria required for the heat and moisture transfer within green roof systems (Burch & Chi, 1997; Delgado et al., 2012; TenWolde, 2011). Among the approved tools, the WUFI simulation software has been chosen for further use by researchers to simulate the bond between moisture and heat conditions through green roof layers owing to some reasons including higher accuracy of hygrothermal simulation results in comparison with experimental measurements under different climate conditions over a long-period monitoring (Künzel, 1994). The rainwater reception and water drainage effect through the greenery layers are other advantages of WUFI simulation software (Schafaczek & Zirkelbach, 2013; Zirkelbach et al., 2017). In addition to the above, the material parameters including liquid water transport, water content, and relative humidity can be easily measured in lab-scale and then introduced into the WUFI software to consider the initial hygrothermal conditions of green roof layers (Zirkelbach, 2017).

The indicators for thermal insulation performance have been attributed to the temperature distribution through materials' depth (Cascone, 2019; Kazemi & Courard, 2020, 2021; Ling et al., 2016). Although some researches have been carried out on green roof systems' insulation performance, few studies have assessed and simulated the hygrothermal conditions of green roof layers, mainly including coarse recycled materials. Also, the optimization of substrate and drainage layers with recycled coarse aggregate has rarely been assessed so far. There are no European standards to propose the optimum thickness for green roof layers concerning their thermal performance (Bellazzi et al., 2020; Saadatian et al., 2013). Therefore, there is a demand for evaluating the thermal resistance of substrate and drainage layers with coarse recycled materials based on their hygrothermal properties.

In this study, the thermal resistance of green roof with substrate of coarse recycled material and the drainage layer of recycled coarse aggregate was tested and evaluated concerning ISO 9869-1 (2014). After that, the heat and moisture properties of green roof layers were introduced into WUFI software and then the modeling outputs were compared and validated with experimental results. Later on, the temperature distribution through the depth of green roof layers was assessed once the thickness of substrate and drainage layers was numerically changed. Finally, the optimum thicknesses of green roof models with a reliable thermal performance were introduced.

Methodology

The initial heat and moisture conditions of substrate and drainage layers based on recycled coarse materials were obtained to assess green roof models' thermal performance. The substrate without recycled coarse aggregate in wet condition and the drainage layer of natural coarse aggregate were considered for the green roof specimen as a control specimen (Fig. 1). Later on, the light substrate produced by Zincohum containing recycled tiles and bricks in wet condition was used for the green roof system once the recycled coarse aggregate was considered for the drainage layer (Fig 2). The maximum size of natural and recycled coarse aggregates for the drainage layer was 7 mm. Fig. 3 shows a cross-sectional view of green roof layers.

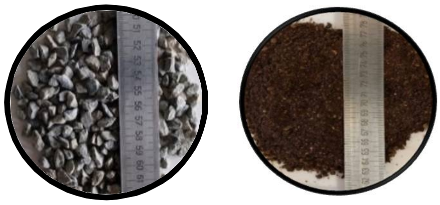

(a) (b)

Fig. 1. Conventional materials for the control green roof specimen: natural coarse aggregate for the drainage layer (a); substrate without recycled coarse aggregate (b).

(a) (b)

Fig. 2. Recycled materials for the green roof specimen: recycled coarse aggregate for the drainage layer (a); substrate containing recycled tiles and bricks (b).

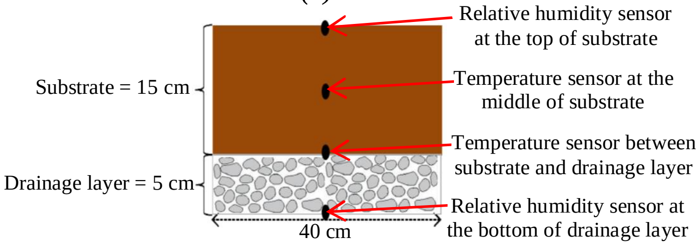

Fig. 3. A cross-sectional view of green roof layers.

The control and proposed green roof specimens were separately put in a 40 × 40 × 20 cm mini experimental mold. After that, the mold was placed in the center of the thermal device between the cooling and heating sides (Fig. 4). The polyurethane foam was used to insulate the mini experimental green roof mold's surrounding area as shown in Fig. 4. The bottom and top of the specimens above was exposed to the temperatures. This device measured the thermal conductivity of green roof layers using a sensor installed in its bottom.

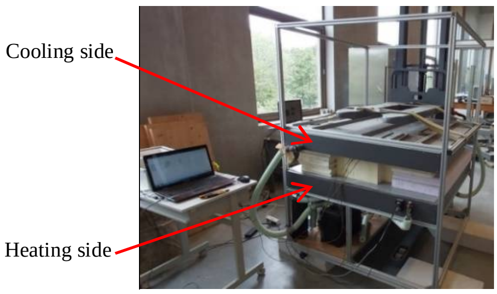

Fig. 4. Thermal device.

The thermal conductivity value (λ) was automatically measured by the thermal device (Fig. 3(b)). Eq. (1) presents the difference between the top and bottom surfaces of specimen (ΔT):

$$\Delta T = T_h - T_c \quad (1)$$

where T_h and T_c are the temperatures in the thermal device's heating and cooling sides, respectively (K).

According to Fourier's law, the density of heat flow rate (q) with the unit of W/m^2 was calculated using Eq. (2):

$$q = \lambda . \frac{\Delta T}{l} \quad (2)$$

where *l* is the thickness of green roof layers (m).

Then, Eq. 3 was used to evaluate the convergence of R_c-value (m^2K/W) using the Average Method given by ISO 9869-1 (2014).

$$R_c = \frac{\sum_{t=0}^{m} \Delta T^t}{\sum_{t=0}^{m} q^t} \quad (3)$$

where *t* is the time interval, and *m* is the minimum required measurement period (h).

To report an acceptable R_c-value based to the Average Method, three main criteria to fulfill and stop the measurement have to include the following:

- The measurement period should take at least 72 h.
- The value calculated at the end of the data set should not deviate more than ±5% from the respective value obtained 24 h before.
- The resulting value when applying the method to the first 67% of data should not deviate by more than ±5 % from the respective value when analyzing the last 67% of the data.

To converge R_c-value using the Average Method given by ISO 9869-1 (2014), it has been recommended that the difference between exterior and interior surface temperature should be considered higher than 3 K (Atsonios et al., 2017). Also, this surface temperature difference should be at least 5-10 K once using the Average Method (Desogus et al., 2011; ISO 9869-1, 2014; Rodler et al., 2019). Therefore, the top and bottom of green roof specimens were subjected to 16.5 K and 23.5 K, respectively, resulting in the surface temperature difference of 7 K.

Concerning the moisture properties of materials, the gravimetric analysis was used for obtaining the water content and relative humidity of substrate and drainage layers, following NF ISO 16586 (2003). As per the criteria given by NF ISO 16586 (2003), the soil should be dried using the oven at 105°C for 48 h.

For green roof layers modeling, the WUFI simulation software was used, and the green roof specimens were exposed to the top and bottom temperatures (temperatures of cooling and heating sides in Fig. 4). In addition, two sensors for measuring the relative humidity of air near to the top and bottom of green roof specimen was installed as shown in Fig. 3. These measured relative humidity at the top and the bottom of the system was also applied to the top and bottom of green roof models.

On the other hand, two sensors for measuring the temperature were installed at the middle of the substrate and between the substrate and drainage layer (Fig. 3). The measurement accuracy of the sensors was ±0.1 °C. For the validation of modeling outputs with experimental results, these two temperatures at a depth of green roof layers were compared with green roof models. After that, since the indicators for thermal insulation performance have been attributed to the temperature distribution through the depth of materials (Cascone, 2019; Kazemi & Courard, 2020; Ling et al., 2016), the temperature values were assessed by changing the thickness of substrate and drainage layers to introduce suitable designs for green roof layers.

Properties and geometrical characteristics of green roof layers

The properties of substrate and drainage layers are presented in Table 1. Each layer's thermal conductivity was separately measured according to ISO 9869-1 (2014) using the thermal device as indicated in Fig. 4. The water vapour diffusion resistance factor (μ) represents the ratio of the diffusion coefficients of water vapor in air and the building material. For very permeable materials such as coarse aggregate layers, the μ-value could be close to 1 (Krus, 1996). The diffusion coefficient of water vapor in the substrate was measured using the cup method adapted to EN 1015 (1999). After that, the μ-value substrate with and without of recycled coarse materials was 3.62 and 3.35, respectively. The free water content of different materials was obtained using the laboratory's gravimetric method based on NF ISO 16586 (2003). The water absorption coefficient of substrate and coarse aggregate was measured and calculated according to EN 1925 (1999). The specific heat capacity of different materials was obtained using the Calorimetric method, which was compatible with ASTM D-16 (2018).

The details and geometrical characteristics of green roofs are presented in Table 2. First, the control green roof specimen including 15-cm substrate without coarse recycled materials and 5-cm drainage layer of natural coarse aggregate (S15-D5-C) was put in the center of the thermal device, and it was exposed to the temperatures from the cooling and heating sides (Fig. 4) for 7 days. After that, the proposed green roof specimen, including 15-cm substrate without coarse recycled materials and 5-cm drainage layer of recycled coarse aggregate (S15-D5) was tested using the thermal device. Later on, the specimens above (S15-D5-C and S15-D5) were modeled and the properties of their layers, presented in Table 1, were introduced to WUFI software. After validation of green roof models with experimental outputs, the effect of the thickness of substrate and drainage layers on the temperature distribution through the depth of green roof models was assessed: by keeping constant the thickness of the substrate, the thickness of drainage layer was changed to 4, 6, 7, and 8 cm for both control and proposed green roof models. In the next step, by keeping constant the thickness of the drainage layer, the substrate's thickness was changed to 12, 18, and 21 cm. Finally, by keeping the percentage of substrate to drainage layer (3) constant, the thicknesses of substrate and drainage layer were changed as presented in Table 2.

Table 1. Properties of green roof layers.

Materials	Bulk density, ρ_s (kg/m^3)	Porosity	Specific heat capacity, Dry (J/kg K)	Thermal conductivity, Dry, λ (W/m·K)	Water vapour diffusion resistance factor, μ	Reference water content (kg/m^3)	Free water content (kg/m^3)	Water absorption coefficient (kg/m^2·s$^{0.5}$)	Typical Built-in moisture (kg/m^3)
Substrate without coarse recycled materials	1075.23	0.482	880	0.15	3.62	10.31	380.95	0.47	125.46
Substrate with coarse recycled materials	1000.95	0.4863	810	0.17	3.35	2.73	285.71	0.22	87.35
Natural coarse aggregate	1436.56	0.4167	770	0.114	1	1.159	42.86	0.0256	4.21
Recycled coarse aggregate	1164.47	0.4956	730	0.11	1	3.321	122.76	0.072	14.34

Table 2. Details and geometrical characteristics of green roofs

No.	Specimen	Substrate		Drainage layer		Thickness (cm)	
		Without coarse recycled materials	With coarse recycled materials	Natural coarse aggregate	Recycled coarse aggregate	Substrate	Drainage layer
1	S[a]15-D[b]4-C[c]	✔	-	✔	-	15	4
2	S15-D5-C	✔	-	✔	-	15	5
3	S15-D6-C	✔	-	✔	-	15	6
4	S15-D7-C	✔	-	✔	-	15	7
5	S15-D8-C	✔	-	✔	-	15	8
6	S12-D5-C	✔	-	✔	-	12	5
7	S18-D5-C	✔	-	✔	-	18	5
8	S21-D5-C	✔	-	✔	-	21	5
9	S12-D4-C	✔	-	✔	-	12	4
10	S18-D6-C	✔	-	✔	-	18	6
11	S21-D7-C	✔	-	✔	-	21	7
12	S15-D4	-	✔	-	✔	15	4
13	S15-D5	-	✔	-	✔	15	5
14	S15-D6	-	✔	-	✔	15	6
15	S15-D7	-	✔	-	✔	15	7
16	S15-D8	-	✔	-	✔	15	8
17	S12-D5	-	✔	-	✔	12	5
18	S18-D5	-	✔	-	✔	18	5
19	S21-D5	-	✔	-	✔	21	5
20	S12-D4	-	✔	-	✔	12	4
21	S18-D6	-	✔	-	✔	18	6
22	S21-D7	-	✔	-	✔	21	7

[a] Substrate
[b] Drainage layer
[c] Control specimen

Results

Comparison between experimental and modelling results

Figs. 5 and 6 show the temperature and relative humidity fluctuations for the control and proposed green roofs. To validate the modeling outputs with experimental results, the temperature variations in the depth of green roof models were compared with those of green roof specimens. The temperature fluctuation at the top and bottom of green roof specimens was nearly the same for the green roof models. After convergence of temperature for the control specimen, the average temperature in the middle of the substrate and between the substrate and drainage layer was 19.64 °C and 21.56 °C, respectively. The corresponding value for the control green roof model was 19.57 °C and 21.5 °C. Therefore, the modeling temperatures were found to be very close to those of experimental results. For the proposed green roof specimen, the average temperature in the middle of the substrate and between the substrate and drainage layers was 19.1 °C and 20.84 °C, respectively. These values for green roof model were equal to 19.05 °C and 21.19 °C. According to the results, the average temperature in the middle of the substrate for the proposed green roof model was nearly the same as the experimental specimen. Moreover, this value between the substrate and drainage layer of the model was 1.7 % more than that of green roof specimen. Therefore, the control and proposed models (S15-D5-C and S15-D5) reliably predicted the temperature distributions through the depth of experimental green roof layers.

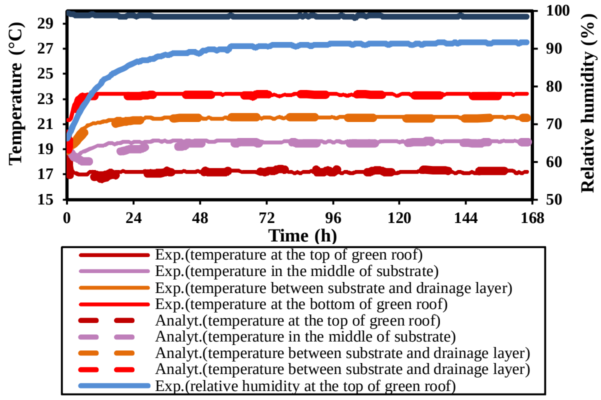

Fig. 5. Experimental results of control green roof specimen (S15-D5-C) and its modeling outputs.

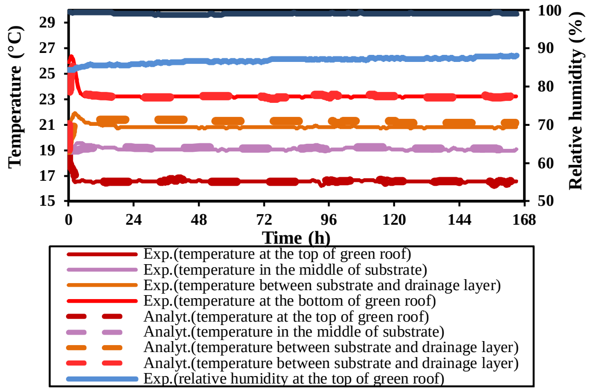

Fig. 6. Experimental results of the proposed green roof specimen with coarse recycled materials (S15-D) and its modeling outputs.

Thickness of drainage layer

Fig. 7 shows the average temperature through the depth of green roof layers with different thicknesses of drainage layer during the last 5 days of the testing period (convergence period of R_c-value). To assess the thickness effect of the drainage layer, the temperature between the substrate and drainage layer for different models was compared. Since the location between substrate and drainage layer was near to the heating side of the thermal device, it was expected that the temperature in this location decreased by increasing the thickness of the drainage layer. Moreover, the thickness could be considered an optimum design for drainage layer once the temperature didn't change. For the control model, the temperature between substrate and drainage layer for green roofs with 4-, 5-, 6-, 7-, and 8-cm drainage layer was obtained 21.82 °C, 21.5 °C, 21.3 °C, 21.27 °C, and 21.2 °C, respectively. This showed a mild decrease in temperature by increasing the thickness of drainage layer of natural coarse aggregate and the temperature for 6-cm drainage layer was obtained nearly the same as 7- and 8-cm drainage layer. On the other hand, this temperature for the proposed green roofs with 6-, 7-, and 8-cm drainage layer was near to 21 °C.

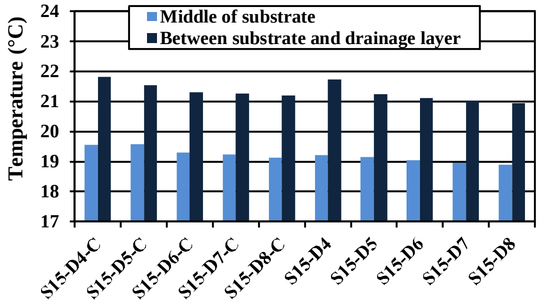

Fig. 7. Temperature in the depth of green roof models with different thicknesses of the drainage layer.

Thickness of substrate

The average temperature through the depth of green roof layers with different substrate thicknesses during the last 5 days of the testing period is shown in Fig. 8. To evaluate the thickness influence of substrate layer, the middle of substrate temperatures for different green roof models were compared to each other. Since the location in the middle of the substrate was near to the cooling side of the thermal device, it was expected that the temperature in this location increased by increasing the thickness of the substrate. Moreover, the thickness could be considered as an optimum design for the substrate once the temperature didn't change after that. According to the modeling outputs, the middle of the substrate's temperature for the control model with 12-cm substrate was 19.28 °C. The approximate value of 19.5 °C was attained for the model with the 15-cm substrate. The temperature above was near to 19.7 °C for the models with 18- and 21-cm substrate. On the other hand, the middle of substrate temperature for the proposed model with 12- and 15-cm substrate was 18.99 °C and 19.1 °C, respectively. However, this value for the proposed model with 18- and 21-cm substrate was about 19.32 °C. As per the results, the proposed model's temperature with 18-cm substrate (S18-D5) was nearly the same as that of the proposed model with 21-cm substrate (S21-D5). The same result was nearly obtained for the control model.

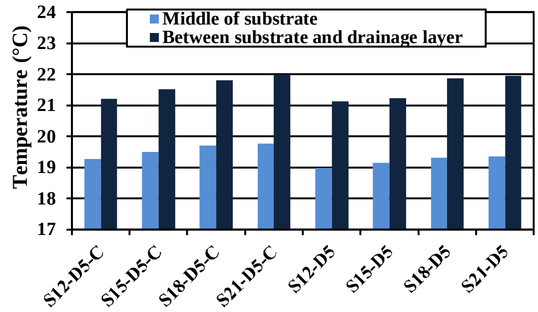

Fig. 8. Temperature in depth of green roof models with different thicknesses of substrate.

Thickness with constant ratio of substrate to drainage layer

Fig. 9 indicates the temperature distribution through the depth of green roof models with constant thickness ratio of substrate to drainage layer during the last five days of the testing period. Since the thicknesses of both substrate and drainage layers were changed, the temperature either in the middle of substrate or between substrate and drainage layer was expected to be affected by the thermal device's cooling and heating sides (Fig 4). According to the results, there was no significant difference in the temperature generated in the middle of substrate layer once the thickness of substrate and drainage layers simultaneously increased. For instance, the range of temperature in the middle of substrate and drainage layer for the control models was 19.4-19.5 °C. The corresponding range for the proposed models was 19.1-19.2 °C. However, there was a moderate increase in the temperature between substrate and drainage layer for both control and proposed models once the thickness of substrate and drainage layers simultaneously increased, even though this temperature for the models with 18-cm substrate was obtained nearly the same as the models with 21-cm substrate. The same results were observed for the models with 12-cm and 15-cm substrate. For example, the temperature between substrate and drainage layer for the proposed model with 12-cm substrate and 4-cm drainage layer (S12-D4) was near 21.2 °C, similar to what was obtained for the proposed model with 15-cm substrate and 5-cm drainage layer (S15-D5). The proposed model's corresponding temperature with 18-cm substrate and 6-cm drainage layer (S18-D6) and the model with 21-cm substrate and 7-cm drainage layer (S21-D7) was near to 21.6 °C.

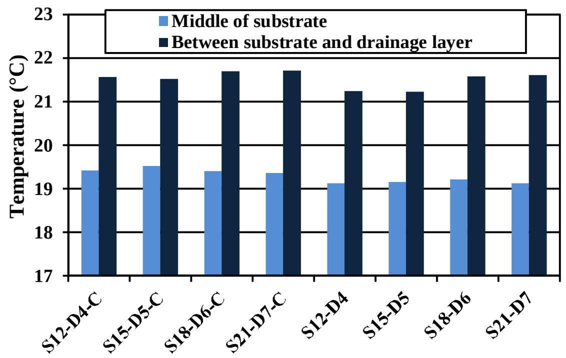

Fig. 9. Temperature in depth of green roof models with constant ratio of substrate to drainage layer.

Discussion

Insulation performance of green roof specimens

Fig. 10 shows the R_c-values of control and proposed green roof specimens, calculated using Eq. 2 to assess their thermal resistance. According to the criteria of Average Method given by ISO 9869-1 (2014), the minimum measurement period should take at least 72 h (3 days). In this regard, the testing period was considered 7 days, and its last 5 days were assumed for the assessment of other criteria given by ISO 9869-1 (2014). R_c-values for the control and proposed green roof specimens were obtained 0.75 m^2K/W and 0.72 m^2K/W, respectively, at the end of the data set. The corresponding values, 24 h before the end of the data set, were 0.743 m^2K/W and 0.713 m^2K/W. By comparing the results, the difference between R_c-values at the end of the test and 24 h before the end of the data set were lower than 1%. Therefore, the R_c-value obtained from the last two measurement days for both control and proposed green roof specimens didn't differ by more than 5%. For the previous 5 days of the testing period, the first and last 67% of R_c-value for the control green roof specimen was on average, about 0.748 m^2K/W and 0.746 m^2K/W, respectively. The corresponding value for the proposed green roof specimen was obtained 0.715 m^2K/W and 0.724 m^2K/W. So, the first and last 67% of R_c-values didn't deviate by more than ±5 %. Generally, it can be considered that the convergence of the R_c-values graph occurred and the results obtained for green roof specimens were compatible with ISO 9869-1 (2014). On the other hand, the results showed that control specimen's Rc-value at the end of the data set was only 4.1% more than that of the proposed specimen. Therefore, there was no significant difference between the control and proposed green roof specimens and thermal resistance of green roof with recycled coarse aggregate was nearly the same as that of green roof without recycled coarse aggregate.

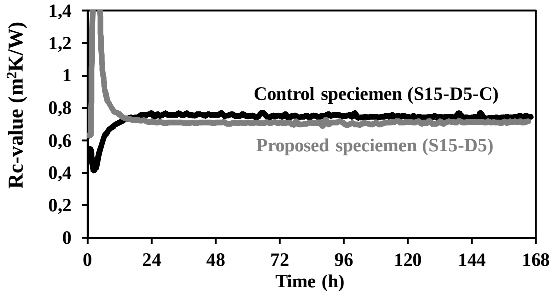

Fig. 10. Experimental results of green roof specimens with coarse recycled materials.

Parametric study

The temperature between the substrate and drainage layer for the green roofs with 6-, 7-, and 8-cm drainage layer was near to each other once the thickness of substrate was assumed to be constant (15 cm). It can be stated that the green roof with a 6-cm drainage layer of natural or recycled coarse aggregate can be considered as optimum design of green roof system. Also, the thermal conductivity of recycled coarse aggregate (0.11 W/m·K) was near natural coarse aggregate (0.114 W/m·K) as presented in Table 1. That is why either the 6-cm natural or recycled coarse aggregate layer (S15-D6-C and S15-D6) allowed to achieve a stable temperature for green roof models.

The temperature in the middle of substrate for green roofs with 18- and 21-cm substrate was near to each other once the thickness of drainage layer was kept to be constant (5 cm). Therefore, the models with 18-cm substrate (S18-D5 and S18-D5-C) can be introduced as optimum green roof designs. This manner showed that the use of coarse recycled materials in the substrate layer provided adequate thermal retention capacity of green roof models due to their great porosity (Zengfeng et al., 2020). Also, the proposed green roof with lower thickness of substrate (S18-D5) applied lower weight to the top of houses and buildings, which can be considered as a benefit from a structural point of view.

By keeping constant the thickness of the substrate, the green roof with 18-cm substrate and 6-cm drainage layer can be considered an optimum design either for the control (S18-D6-C) or for the proposed model (S18-D6). It is noteworthy that researchers (Rincón et al., 2014; Sadeghian et al., 2020) have proposed to select the roof with a lighter weight for buildings and houses. This means that using the proposed model (S18-D6) for rooftop is recommended because of its lower weight than the control model (S18-D6-C).

Another point is that the optimum designs of the control model were S15-D6-C and S18-D5-C once the thickness of the drainage layer and substrate separately increased. In contrast, S18-D6-C was considered an optimum design of control model once the thickness of drainage layer and substrate simultaneously increased. The simultaneous increase in thickness of substrate and drainage layer led to their better participation for generating the thermal resistance for the green roof system. Considering the density of natural coarse aggregate and substrate without coarse recycled materials presented in Table 1, among optimum designs for the control model, S15-D6-C with 247.48 kg/m^2 had the lowest weight. On the other hand, among the proposed model's optimum designs, the lowest weight was observed for S15-D6 with the weight of 220.01 kg/m^2. Generally, coarse recycled materials for green roof layers are recommended to be developed in the construction sector, due to their adequate thermal resistance and low weight.

Conclusions

The thermal performance of green roof layers with coarse recycled materials was assessed once their initial heat and moisture properties were simultaneously considered and modeled. The following conclusions can be drawn from experimental results and modeling outputs:

The convergence of the R_c-value graph was achieved based on ISO 9869-1 (2014), where this value for the control specimen at the end of the data set was slightly higher than that of the control specimen (4.1%), indicating nearly the same thermal resistance of the former and the latter.

The thermal performance of green roof layers with and without coarse recycled materials was reliably modeled and predicted after introducing the initial hygrothermal properties of substrate and drainage layers into WUFI software. Moreover, the temperature distribution graphs in the depth of green roof models remained stable and similar to those observed for the lab-scale green roof specimens.

The 6-cm drainage layer of natural or recycled coarse aggregate were introduced as optimum thicknesses for the control (S15-D6-C) and proposed (S15-D6) models, respectively, once the thickness of substrate layer remained constant (15 cm). On the other hand, the control and the proposed models with 18-cm substrate (S18-D5-C and S18-D5) were introduced as optimum green roof designs once the thickness of drainage layer was kept constant (5 cm).

By keeping constant the thickness ratio of substrate to drainage layer (3), the model with 18-cm substrate and 6-cm drainage layer can be considered as an optimum design either for the control (S18-D6-C) or for the proposed model (S18-D6).

Among the models with optimized thicknesses, S15-D6-C and S15-D6 were considered the best designs for the control and the proposed green roofs, respectively, because of their adequate thermal resistance and lower weight.

Acknowledgement

This research was funded through the University of Liège (ULg) and ARC grant for Concerted Research Actions, financed by the French Community of Belgium, Wallonia-Brussels Federation (CityRoof project: *Analogous green roofs for urban ecosystem services* (2020-2023)).

References

ASTM D4611 - 16. (2018). *Standard test method for specific heat of rock and soil*. ASTM International.

Atsonios, I. A., Mandilaras, I. D., Kontogeorgos, D. A., & Founti, M. A. (2017). A comparative assessment of the standardized methods for the in–situ measurement of the thermal resistance of building walls. *Energy and Buildings*, *154*, 198–206.

Bellazzi, A., Barozzi, B., Pollastro, M. C., & Meroni, I. (2020). Thermal resistance of growing media for green roofs: To what extent does the absence of specific reference values potentially affect the global thermal resistance of the green roof? An experimental example. *Journal of Building Engineering*, *28*, 101076.

Berndtsson, J. C., Emilsson, T., & Bengtsson, L. (2006). The influence of extensive vegetated roofs on runoff water quality. *Science of the Total Environment*, *355*(1–3), 48–63.

Burch, D. M., & Chi, J. (1997). MOIST: A PC program for predicting heat and moisture transfer in buildingenvelopes. Release 3.0. *NIST Special Publication*, *917*.

Cascone, S. (2019). Green Roof Design: State of the Art on Technology and Materials. *Sustainability*, *11*(11), 3020. https://doi.org/10.3390/su11113020

Cascone, S., Catania, F., Gagliano, A., & Sciuto, G. (2018). A comprehensive study on green roof performance for retrofitting existing buildings. *Building and Environment*, *136*, 227–239.

Chenani, S. B., Lehvävirta, S., & Häkkinen, T. (2015). Life cycle assessment of layers of green roofs. *Journal of Cleaner Production*, *90*, 153–162.

Coma, J., Pérez, G., Castell, A., Solé, C., & Cabeza, L. F. (2014). Green roofs as passive system for energy savings in buildings during the cooling period: Use of rubber crumbs as drainage layer. *Energy Efficiency*, *7*(5), 841–849.

Coma, J., Pérez, G., Solé, C., Castell, A., & Cabeza, L. F. (2016). Thermal assessment of extensive green roofs as passive tool for energy savings in buildings. *Renewable Energy*, *85*, 1106–1115.

Delgado, J. M., Barreira, E., Ramos, N. M., & De Freitas, V. P. (2012). *Hygrothermal numerical simulation tools applied to building physics*. Springer Science & Business Media.

Desogus, G., Mura, S., & Ricciu, R. (2011). Comparing different approaches to in situ measurement of building components thermal resistance. *Energy and Buildings*, *43*(10), 2613–2620.

Dvorak, B., & Volder, A. (2013). Rooftop temperature reduction from unirrigated modular green roofs in south-central Texas. *Urban Forestry & Urban Greening*, *12*(1), 28–35.

EN 1015-19. (1999). *Methods of test for mortar for masonry. Determination of water vapour permeability of hardened rendering and plastering mortars*.

EN 1925. (1999). *Natural stone test methods. Determination of water absorption coefficient by capillarity*.

ISO 9869-1. (2014). 9869-1: 2014 Thermal insulation, Building elements, In-situ measurement of thermal resistance and thermal transmittance-Part 1: Heat flow meter method. *London: BSI*.

ISO 16586. (2003a). *Soil quality—Determination of soil water content as a volume fraction on the basis of known dry bulk density—Gravimetric method*. ISO. https://www.iso.org/cms/render/live/en/sites/isoorg/contents/data/standard/03/23/32317.html

ISO 16586. (2003b). *Soil quality—Determination of soil water content as a volume fraction on the basis of known dry bulk density—Gravimetric method*. ISO. https://www.iso.org/cms/render/live/en/sites/isoorg/contents/data/standard/03/23/32317.html

Jim, C. Y. (2014). Air-conditioning energy consumption due to green roofs with different building thermal insulation. *Applied Energy*, *128*, 49–59.

Kazemi, M., & Courard, L. (2020). Modelling thermal and humidity transfers within green roof systems: Effect of rubber crumbs and volcanic gravel. *Advances in Building Energy Research*, *0*(0), 1–26. https://doi.org/10.1080/17512549.2020.1858961

Kazemi, M., & Courard, L. (2021). Simulation of humidity and temperature distribution in green roof with pozzolana as drainage layer: Influence of outdoor seasonal weather conditions and internal ceiling temperature. *Science and Technology for the Built Environment*, *27*(4), 509–523.

Kazemi, M., Hajforoush, M., Talebi, P. K., Daneshfar, M., Shokrgozar, A., Jahandari, S., Saberian, M., & Li, J. (2020). In-situ strength estimation of polypropylene fibre reinforced recycled aggregate concrete using Schmidt rebound hammer and point load test. *Journal of Sustainable Cement-Based Materials*, 1–18.

Krus, M. (1996). *Moisture transport and storage coefficients of porous mineral building materials: Theoretical principles and new test methods*. Fraunhofer IRB Verlag Stuttgart.

Künzel, H. M. (1994). *Verfahren zur ein-und zweidimensionalen Berechnung des gekoppelten Wärme-und Feuchtetransports in Bauteilen mit einfachen Kennwerten* [PhD Thesis]. Universität Stuttgart Stuttgart.

Ling, H., Chen, C., Qin, H., Wei, S., Lin, J., Li, N., Zhang, M., Yu, N., & Li, Y. (2016). Indicators evaluating thermal inertia performance of envelops with phase change material. *Energy and Buildings*, *122*, 175–184.

Mickovski, S. B., Buss, K., McKenzie, B. M., & Sökmener, B. (2013). Laboratory study on the potential use of recycled inert construction waste material in the substrate mix for extensive green roofs. *Ecological Engineering*, *61*, 706–714.

Nematzadeh, M., Shahmansouri, A. A., & Fakoor, M. (2020). Post-fire compressive strength of recycled PET aggregate concrete reinforced with steel fibers: Optimization and prediction via RSM and GEP. *Construction and Building Materials*, *252*, 119057. https://doi.org/10.1016/j.conbuildmat.2020.119057

Rincón, L., Coma, J., Pérez, G., Castell, A., Boer, D., & Cabeza, L. F. (2014). Environmental performance of recycled rubber as drainage layer in extensive green roofs. A comparative Life Cycle Assessment. *Building and Environment*, *74*, 22–30.

Rodler, A., Guernouti, S., & Musy, M. (2019). Bayesian inference method for in situ thermal conductivity and heat capacity identification: Comparison to ISO standard. *Construction and Building Materials*, *196*, 574–593.

Saadatian, O., Sopian, K., Salleh, E., Lim, C. H., Riffat, S., Saadatian, E., Toudeshki, A., & Sulaiman, M. Y. (2013). A review of energy aspects of green roofs. *Renewable and Sustainable Energy Reviews*, *23*, 155–168.

Sadeghian, F., Haddad, A., Jahandari, S., Rasekh, H., & Ozbakkaloglu, T. (2020). Effects of electrokinetic phenomena on the load-bearing capacity of different steel and concrete piles: A small-scale experimental study. *Canadian Geotechnical Journal*, *ja*.

Schafaczek, B., & Zirkelbach, D. (2013). *Ermittlung von Materialeigenschaften und effektiven Übergangsparametern von Dachbegrünungen zur zuverlässigen Simulation der hygrothermischen Verhältnisse in und unter Gründächern bei beliebigen Nutzungen und unterschiedlichen Standorten:[Abschlussbericht]*. Fraunhofer-IRB-Verlag.

Tabares-Velasco, P. C., Zhao, M., Peterson, N., Srebric, J., & Berghage, R. (2012). Validation of predictive heat and mass transfer green roof model with extensive green roof field data. *Ecological Engineering*, *47*, 165–173.

TenWolde, A. (2011). A review of ASHRAE Standard 160—Criteria for moisture control design analysis in buildings. In *Condensation in Exterior Building Wall Systems*. ASTM International.

Uhl, M., & Schiedt, L. (2008). Green roof storm water retention–monitoring results. *11th International Conference on Urban Drainage, Edinburgh, UK*, *31*.

Vesuviano, G., & Stovin, V. (2013). A generic hydrological model for a green roof drainage layer. *Water Science and Technology*, *68*(4), 769–775.

Vijayaraghavan, K., Joshi, U. M., & Balasubramanian, R. (2012). A field study to evaluate runoff quality from green roofs. *Water Research*, *46*(4), 1337–1345.

Vijayaraghavan, Kuppusamy. (2016). Green roofs: A critical review on the role of components, benefits, limitations and trends. *Renewable and Sustainable Energy Reviews*, *57*, 740–752.

Vila, A., Pérez, G., Solé, C., Fernández, A. I., & Cabeza, L. F. (2012). Use of recycled rubber from tires as drainage layer in green roofs. *Building and Environment*, *48*, 101–106.

Wanielista, M., Kelly, M., & Hardin, M. (2008). A Comparative analysis of greenroof designs including depth of media, drainage layer materials, and pollution control media. *Florida Department of Environmental Protection: Tallahassee, FL, USA*.

Zirkelbach, D. (2017). *Green roofs − hygrothermal simulation of moisture and energy performance*. 6.

Zirkelbach, D., Mehra, S.-R., Sedlbauer, K.-P., Künzel, H.-M., & Stöckl, B. (2017). A hygrothermal green roof model to simulate moisture and energy performance of building components. *Energy and Buildings*, *145*, 79–91.